Lg **wave attenuation in Britain**

Susanne Sargeant [*] and Lars Ottemöller

SUMMARY

The Lg wave quality factor (Q_{Lg}) in Britain has been modelled using data from the UK Seismic Network, operated by the British Geological Survey. The dataset consists of 631 vertical, mostly short-period recordings of Lg waves from 64 earthquakes (2.7-4.7 ML) and 93 stations. We have inverted for both regional average Q_{Lg} and tomographic images of Q_{Lg}, and simultaneously a source term for each event and a site term for each station for 22 frequencies in the band 0.9-10.0 Hz. The regional average model is $266f^{0.53}$ between 1.0 and 10.0 Hz and indicates that attenuation in Britain is slightly higher than in France, and significantly higher than in eastern North America and Scandinavia. Tomographic inversions at each frequency indicate that Q_{Lg} varies spatially. Broadly speaking, south-eastern England, the Lake District and parts of the East Irish Sea Basin, and a small region between the Highland Boundary Fault and the Southern Uplands Fault are characterised by higher than average attenuation. South-western England, eastern central England and north-western Scotland are regions of relatively low attenuation. To some extent, these regions correlate with what is known about the tectonics and structure of the crust in the UK.

Key words: Attenuation, British Isles, crustal structure , Lg wave, quality factor, tomography

[*]British Geological Survey, Murchison House, West Mains Road, Edinburgh, United Kingdom, Tel: +44 (0)131 6500245, Fax: +44 (0)131 6671877, Email: s.sargeant@bgs.ac.uk

2   *S. Sargeant and L. Ottemöller*

1   INTRODUCTION

Material and physical properties of the Earth's interior can be inferred from measurements of attenuation (Aki, 1980). Lg waves (multiply reflected shear waves) are almost routinely used to study the crustal quality factor, Q_{Lg}, which is a direct measure of attenuation. The attenuation of Lg and its correlation with large scale crustal features has been described by numerous authors including Kennett (1986), Mitchell and Hwang (1987), Bowman and Kennett (1991), Campillo and Plantet (1991), Mitchell et al. (1998) and Baumgardt (2001). These studies demonstrate that Lg wave attenuation is strongly correlated with the age of the crust, variations in crustal thickness, the nature of the crust-mantle transition, sediment thickness and crustal complexity.

There are few published studies of seismic wave attenuation in Britain and none that investigate attenuation of Lg waves. MacBeth and Burton (1987) determined Q_β along single source-station paths using data from small underground and underwater explosions in Scotland recorded at epicentral distances of up to 85 km. They found no noticeable correlation between the variation in the single station values and surface geology. Scheirer and Hobbs (1990) studied crustal attenuation off the south-west coast of England using deep seismic reflection data. They observed that the thick granite plutons present in this region are associated with relatively low attenuation. The most recent attenuation model is presented by Edwards et al. (2008). In this study, source, path and site effects were determined from S wave recordings of small to moderate magnitude earthquakes in the UK. The data were also inverted for geometrical spreading using a multiple segment geometrical spreading function. Edwards et al. (2008) found that a frequency independent and depth dependent Q in the range of about 920 at the top of the crust and 5700 in the deeper crust best explains the data. Site amplification and kappa were found to correlate with site geology.

In contrast to Britain, neighbouring areas of north-western Europe are comparatively well studied in terms of Lg wave attenuation. In France, investigations include Campillo et al. (1985), Campillo (1987) and Campillo and Plantet (1991). In Scandinavia, Q_{Lg} has been examined by Kvamme et al. (1995). Lg wave propagation in the North Sea has received much attention and the Central and Viking grabens are known to be major barriers to efficient Lg wave propagation (Kennett and Mykkeltveit, 1984; Gregersen and Vaccari, 1993; Furumura and Kennett, 1997).

Our primary objective in this study is to increase the understanding of Lg wave propagation and how it relates to crustal structure in Britain. In doing so, we seek to provide information on attenuation, which is needed for reliable prediction of ground motion from future British earthquakes. To this end, regional average Q_{Lg} was determined and tomographic inversions in the frequency range 1.0-10.0 Hz were performed to map the lateral variations in Q_{Lg}. This is the first study to present a regional average frequency-dependent Q model and to describe the spatial variations in Lg wave attenuation across Britain.

There are inadequacies in the way in which local magnitude (ML) is computed, particularly for poorly recorded small earthquakes or larger earthquakes with limited numbers of on-scale records. As pointed out by Deichmann (2006), there is a requirement for more robust methods for quantifying earthquake size, such as spectral measurements of moment magnitude (MW). Furthermore, ground motion relations are increasingly given in terms of MW. This adds to the need for MW to be routinely determined rather than estimated via some empirical relation that relates potentially unreliable estimates of ML to MW and will contain its own uncertainties (Deichmann, 2006). Therefore a secondary objective of this study is to use the obtained Q_{Lg} and determine MW for the earthquakes in the dataset to investigate the relationship between ML and MW.

2   TECTONICS

The crust of Britain and Ireland can be divided into three main blocks (Figure 1): (1) the Laurentian crustal block which underlies most of northern Scotland; (2) the Avalonian/Gondwana crustal block of southern Britain; and (3) an intervening zone of accreted terranes, forming a complex collision zone which separates the remains of the Laurentian and Avalonian/Gondwana continental masses. The assemblage of these crustal blocks can be related to the closure of the Iapetus Ocean during the Ordovician to late Silurian (460 to 420 Ma). The main boundary between these two continental masses, the Iapetus Suture, runs through the Solway Firth (Figure 1), essentially along the border between Scotland and England. This is arguably the most fundamental structural lineament in Britain and Ireland (Beamish and Smythe, 1986). The suture is nowhere exposed but can be clearly seen on seismic profiles, and is associated with a short wavelength increase in Moho depth of about 5 km relative to the area outside the suture zone (Chadwick and Pharaoh, 1998).

4   *S. Sargeant and L. Ottemöller*

The Laurentian crustal block of northern Scotland consists of the metamorphosed Precambrian rocks of the Hebridean, Northern Highlands and Central Highlands terranes (Figure 1). The Hebridean terrane includes the oldest rocks exposed in the British Isles. The southern margin of the Laurentian crustal block is formed by the Highland Boundary Fault. This fault has had a prolonged and complex history of movement and is interpreted as a major terrane boundary. Small earthquakes in this fault system indicate that, at present, it accommodates only minor local stress adjustments (Ottemöller and Thomas, 2006).

The complex collision zone that underlies much of southern Scotland and northern England consists of a number of broadly NE-SW-trending elongate terranes, which were accreted to the southern Laurentian continental margin during the closure of Iapetus Ocean (Cocks, 2005). The most northerly of these terranes is the Midland Valley, which comprises a complex assemblage of ophiolitic, sedimentary and volcanic rocks. South of the Midland Valley is the Southern Uplands terrane (SUT) (Figure 1), which is made up of rocks deposited in either a trench associated with NW-directed subduction (e.g., Leggett et al. , 1979), or back-arc to foreland thrust basin (e.g., Stone et al. , 1987). The SUT is bounded to the south by the Iapetus Suture.

The Avalonian crust south of the suture is characterised by lower velocities than the Laurentian block (Clegg and England, 2003). The Leinster-Lakesman terrane consists of sedimentary and volcanic rocks that record the development of volcanic arc and fault-controlled marginal basins along the northern margin of eastern Avalonia, during subduction along the southern margin of the Iapetus Ocean (Clegg and Holdsworth, 2005). In central and eastern England, the Caledonian metamorphic basement is largely concealed by late Palaeozoic, Mesozoic and Cenozoic strata (Pharaoh et al. , 1995; Green et al. , 2001). Southern England is dominated by the allochthonous fold-thrust belt of the Variscan Rhenohercynian Zone which formed during the closure of the Rheic Ocean in the Carboniferous (Chadwick and Pharaoh, 1998).

3 DATA

The data used in this study were from the seismic network operated by the British Geological Survey (BGS) and restricted to events recorded between January 1984 and April 2007. The greatest concentration of stations is in western Britain where levels of seismicity are highest. The data are mostly from Willmore Mk III sensors but there are also several records from broadband instruments. Clipping is a problem for the short-period data as it is recorded on low dynamic range systems and we excluded all saturated recordings after visual inspection. Station locations are shown in Figure 2 a. Crustal earthquakes were selected for the area -7.5 to 2.5 °E and 48 to 59 °N. This region encloses much of Britain and the Irish Sea. We required that earthquakes were recorded at a minimum of four stations and at distances between 170 km and 600 km. Furthermore, we required a minimum of four earthquakes recorded at each station. The minimum distance is set to twice the critical distance for SmS. In the UK, where the crust is 30-35 km thick (Chadwick and Pharaoh, 1998), this is 170 km. Sn coda contamination can have a marked effect on determinations of Q_{Lg}, particularly at long distances and high frequencies (Shin and Herrmann, 1987; Adams and Haddon, 1998). To investigate whether this was important for the UK data, seismograms were filtered in various frequency ranges to gauge whether Lg was visible above the coda of Sn. The analysis showed that Lg is the largest amplitude arrival at all frequencies for distances less than 600 km but is not visible in the Sn coda at higher frequencies (> 7 Hz) and longer distances. Consequently, a maximum distance of 600 km was specified for all frequencies. The conditions above were met by 64 events in the range 2.7 to 4.7 ML recorded on 93 stations (see Figure 2 a).

The final dataset consisted of 631 vertical mostly short-period records of Lg. The Lg group velocity range to window the data was selected between 3.7 and 3.0 km/s. The distribution of observations with distance (Figure 2 b) reflects the magnitude content of the dataset: most paths are relatively short (88% are less than 450 km long). The greatest concentration of travel paths is achieved in western and central Britain. In comparison, north-eastern Scotland and the English Channel are relatively poorly sampled.

6   *S. Sargeant and L. Ottemöller*

4   METHOD

Q_{Lg} was derived from the decay of spectral displacement amplitudes with distance for a range of individual frequencies following the method described by Ottemöller et al. (2002). This approach has been successfully applied in southern Mexico (Ottemöller et al. , 2002), Central America (Ottemöller, 2002) and Colombia (Ojeda and Ottemöller, 2002). Regional average Q_{Lg} was determined for 22 frequencies between 0.9 Hz and 10.0 Hz. We simultaneously inverted for the seismic moment for each earthquake and site terms at each station, along with Q_{Lg}. The Lg-wave displacement spectral amplitude $A_{kl}(f)$ for the event k, at the recording site l, after removal of the instrument response, is given by

$$A_{kl}(f) = S_k(f)L_l(f)G(R)exp(-\pi f R Q_{Lg}^{-1}/v) \tag{1}$$

where $S_k(f)$ is the source term, $L_l(f)$ is the local site term, R is the hypocentral distance, v is the average Lg-peak velocity (3.35 km/s), Q_{Lg} is the quality factor, and $G(R)$ is the geometrical spreading ($G(R) = (R_x R)^{-1/2}$ for $R \geq 100$ km, $R_x = 100$ km, Hermann and Kijko (1983)). Taking the logarithm of equation (1) gives

$$logA_{kl}(f) + 0.5log(R_x R) =$$
$$logS_k(f) + logL_l(f) - (\pi f R \, log(e)/v)Q_{Lg}^{-1} \tag{2}$$

As a constraint for the site terms we required that

$$\sum_l logL_l(f) = 0 \tag{3}$$

In the tomograpic inversion, Q_{Lg} is integrated along the travel path and equation 2 becomes

$$logA_{kl}(f,R) + 0.5log(R_x R) + \pi(\sum R_i)flog(e)v^{-1}Q_{Lg\,apriori}^{-1} =$$
$$logS_k(f) + logL_l(f) - (\pi flog(e)v^{-1})\sum(\Delta Q_{Lg\,i}^{-1}R_i) \tag{4}$$

where $\Delta Q_{Lg\,i}$ is the variation from the average $Q_{Lg\,apriori}$ in grid cell i.

To study lateral variations in Q_{Lg}, the region of interest was divided into evenly spaced grid cells. We determined an optimum grid cell size of 89 km in the north-south and east-west directions, which reflected the quality and quantity of the data available. At this grid size, most of onshore Britain is well resolved with the exception of northernmost Scotland. The function to be minimised in the inversion includes a matrix to regularise the mixed-determined problem (Barmin et al. , 2001). The constants in this matrix add spatial smoothness to the Q_{Lg} model and constrain the result to the starting model (the regional average) where ray path coverage is low. We performed a series of checkerboard tests using different combinations of constants in order to determine a suitable combination. That is, the combination that produced models without unrealistic, sharp changes in Q_{Lg} between adjacent cells, and anchored the result to the starting model only in poorly determined grid cells. The optimum constants (following the nomenclature of Ottemöller et al. (2002)) were $\alpha = 500$, $\sigma = 62.5$, $\beta = 1500$ and $\lambda = 0.001$ (Figure 3).

Shifting the grid boundaries in various ways, slightly different tomographic images are obtained. By overlaying and averaging several of these images, it is possible to obtain more complex images with higher nominal resolution, without introducing inversion ambiguities and instabilities (Vesnaver and Böhm, 2000). Here, by overlaying and averaging three grids, it is possible to achieve 45 km grid spacing without compromising the reliability of the results.

While Figure 3 suggests that the inversion can resolve variations in Q_{Lg}, equation 4 shows that there is a trade-off between attenuation, the site terms and the source terms. Menke (2006) provided a practical method to investigate the nonuniqueness between attenuation and the source terms, which allows unresolvable attenuation patterns to be determined. Menke (2006) suggests that the null solutions are computed by applying a perturbation to the source terms individually and then inverting for the attenuation pattern without inverting for the source terms. These null solutions could be added to solutions of equation 4 without changing the equation. We computed the set of inversions for all sources for a constant Q model by perturbing one source at a time by the equivalent of 0.1 and 0.2 moment magnitude units. An example is shown in Figure 4, which shows that an increase to one of the source terms gets mapped into higher Q in grid cells with path coverage. We also see lower Q adjacent grid cells without path coverage. Obviously, the effect is stronger for a larger source size perturbation.

8   *S. Sargeant and L. Ottemöller*

A potential error can be introduced from the measurements of the spectral levels. We tested the effect of this error by adding Gaussian noise amounting to a maximum of 0.1 moment magnitude units. The comparison of results is shown in Figure 5 a and b. The added noise leads to variation in both Q and site term. Another potential error stems from the nonuniqueness involving the site terms. To investigate the significance of the site terms, we performed the tomographic inversion without inverting for the site terms. An example of this inversion for f =4 Hz is shown in Figure 5 c. When not inverting for the site terms we find that grid cells with previously negative site terms and high Q show up with a lower Q when not inverting for the site term and vice versa. This is expected and demonstrates the nonuniqueness between Q and the site terms. However, both the inversion without site term and the noise test show that the inversion is reasonably stable. Later, we determine the site terms using spectral ratio technique to evaluate the site terms independently.

5   RESULTS

5.1   Regional Average Q_{Lg}

The spatial coverage of the data is such that an estimate of regional average Q_{Lg} will be representative of most of onshore Britain. Figure 6 shows Q_{Lg}^{-1} obtained for frequencies between 0.9 Hz and 10.0 Hz. The results are associated with relatively large uncertainties at lower frequencies where the signal strength is poorer for small earthquakes. Q_{Lg} is often related to frequency via the power law of Fedotov and Boldyrev (1969) and Aki (1980):

$$Q_{Lg}(f) = Q_0(f/f_0)^{\eta} \tag{5}$$

It is conventional to take f_0 to be 1 Hz and Q_0 to be equal to Q at 1 Hz (Shi et al. , 1996). Q_{Lg}^{-1} is clearly frequency dependent but the onset of frequency dependence is not clear. Therefore, it is assumed to occur at 1 Hz. Under this assumption, $Q_{Lg} = 266 f^{0.53}$ between 1.0 Hz and 10.0 Hz. This model is also shown in Figure 6.

The inverted site terms vary smoothly with frequency, as shown for the three-component stations in Figure 7 (and labelled on the map in Figure 2). These are the stations for which noise data were available for the additional analysis described below. The results are broadly consistent with the geological information on the station foundation with hard rock sites (EDI, ESK, BBO, MCH, CR2, HPK and CWF) showing little amplification. At stations founded on softer geology (MCD, BHH, SWN and TFO), the effect of the site conditions appears to be stronger. We used the Nakamura or H/V spectral ratio technique (Noghoshi and Igarashi, 1970, 1971; Nakamura, 1989) to empirically estimate the site response at these stations as an independent check of the validity of the results. The technique involves computation of the horizontal to vertical (H/V) spectral ratio from microtremor recordings. The peaks in the H/V ratio are related to sharp impedance contrasts below the recording site. This technique is expected to reveal the fundamental frequencies at which amplification occurs, but not necessarily with the correct amplitudes (e.g., SESAME, 2004; Atakan et al. , 2004). While there are limitations to this method, a great number of field studies suggest that it works (e.g., Konno and Ohmachi, 1998; Sørensen et al. , 2006). The results of the H/V spectral ratio analysis are also shown in Figure 7. The results generally compare well to the inverted site terms for stations founded on hard bedrock. There is a greater deviation, particularly in terms of absolute amplitude, between the H/V spectral ratios and the inverted site terms at stations located on softer deposits like top soil and glacial till. Overall, the results of the H/V spectral ratio technique give us confidence in the inverted site terms.

5.2 Q_{Lg} **Tomography**

We used the average $Q_{Lg}(f)$ model as the a priori information for independent tomographic inversions at the same frequencies. Figure 8 presents the results for 1.0, 1.6, 2.5, 4.0, 6.3 and 10.0 Hz, which show consistent and significant large-scale variations in Q_{Lg}^{-1} in the British Isles. The spatial resolution is of the order of 100-200 km. The best resolved area coincides with the region where ray path coverage is most dense, that is, western Britain. In northernmost Scotland where coverage is sparse, the result is anchored to the starting model. The corresponding site terms recovered from the inversion are shown in Figure 7.

The tomographic images are difficult to interpret. Broadly speaking, six regions can be identified

10   *S. Sargeant and L. Ottemöller*

from the tomographic images. Zone 1: south-eastern England - this is a region of slightly higher than average attenuation (475-500 at 4 Hz). It is bounded by regions of lower than average attenuation to the north and west. Zone 2: south-western England - this is an area of lower than average attenuation. At 4 Hz, Q_{Lg} is of the order of 625. Zone 3 is a region of relatively low attenuation, north of Zone 1 and extending as far west as the Pennines. It is a prominent feature at all frequencies. Both positive site terms and high Q are consistent with low attenuation. This is a system of major basin-controlling normal faults. To the west of this is a region of slightly higher than average attenuation (Zone 4) that covers the Lake District and East Irish Sea Basin. The attenuation characteristics for this region vary with frequency. Zone 5 is a small area of relatively high attenuation. Zone 6 is characterised by lower than average attenuation and covers central and northern Scotland. One might suppose that north-eastern Scotland would also be an area of lower than average attenuation since the crust here is also Laurentian.

5.3 Moment Magnitudes for British Earthquakes (1996-2007)

Using the average $Q_{Lg}(f)$ to correct for attenuation, MW was determined from Lg-wave displacement spectra for each of the earthquakes in the dataset using a converging grid search method (Ottemöller and Havskov, 2003). The source term $S(f)$ in equation 1 for a simple ω^2 model is given by Aki (1967) and Brune (1970, 1971)

$$S(f) = \frac{M_0}{4\pi k \rho v^3} \left[1 + \frac{f^2}{f_c^2} \right]^{-1} \tag{6}$$

where M_0 is the seismic moment, $k = 0.83$ (this factor corrects for free-surface reflection and the radiation pattern), ρ is density, v is the S-wave speed at the source, and f_c is the corner frequency. Since for $f < f_c$ the source spectrum is flat and proportional to M_0, seismic moment can be easily determined from the long period part of the source spectrum. Near surface attenuation, represented by κ, depends on the quality factor in the near surface layers at each station (e.g., Anderson and Hough, 1984). This was not modelled explicitly because near surface attenuation in the UK is not well understood. Furthermore, the inclusion of κ for the average Q_{Lg} model does not modify

the diminution function by a significant amount at the distances and frequencies considered here (generally greater than 100 km). Typical results from the spectral modelling are shown in Figure 9.

The results are shown in Table 1. Calculating MW at individual stations acts as an independent check on the regional average quality factor since it allows us to check for distance dependence, which would imply a deficiency in the attenuation model. Figure 10a shows that when plotted against distance, individual estimates are evenly distributed above and below the average value and are not distance-dependent. Furthermore, MW for the largest earthquake in the dataset (22 September 2002, 4.7 ML, 4.2 ± 0.1 MW) is in agreement with MW determined by ETH Zürich (4.3 MW) from the regional moment tensor.

Figure 10b shows MW plotted against local magnitude (ML) for the earthquakes in our dataset. ML, as calculated by the BGS, is determined from the logarithm of the maximum amplitude recorded on each of two orthogonal horizontal seismometers, correcting for distance (using the correction of Hutton and Boore (1987) for southern California), and taking the mean of the two component magnitudes (Booth, 2007). We obtain the following relationship between ML and MW (Figure 10 b):

$$MW = 0.70\,ML + 0.70 \tag{7}$$

This is almost the same as the relationship determined by Edwards et al. (2008) ($MW = 0.71ML + 0.58$). Further comparison between Edwards et al. (2008) and our results is made in the next section.

6 DISCUSSION

We have determined a regional average frequency-dependent Q_{Lg} model for Britain, which can be used routinely to determine MW from displacement spectra. Comparisons can be made between our attenuation model and models determined for other stable continental regions. Using data from earthquakes in and around Norway, Kvamme et al. (1995) found $Q(f) = 440f^{0.7}$ for Scandinavia

12   *S. Sargeant and L. Ottemöller*

(see Figure 6). Benz et al. (1997) determined $Q(f) = 1052(f/1.5)^{0.22}$ for eastern North America. Both models point to significantly lower attenuation in these regions than in Britain. Campillo and Plantet (1991) proposed $Q_{Lg} = 320f^{0.5}$ for France (see Figure 6). The frequency dependence is similar to what we have found for Britain but the model for France indicates slightly higher Q_0. For comparison, $Q(f) = 187f^{0.55}$ for southern California (Benz et al., 1997).

Our results show that attenuation varies spatially across the British Isles and there are distinct regions of relatively high and low Q. We assume that the differences are real, despite the inherent non-uniqueness problem between Q and the source terms. We had expected there to be some degree of correlation between the tomographic results and the configuration of the tectonic terrains. For example, for the ancient Laurentian terrains north of the Highland Boundary Fault to be characterised by relatively high Q, in line with estimates for eastern North America. Furthermore, our hypothesis was that the accreted terrains of the Midland Valley and the Southern Uplands would be regions of relatively low Q due to the complex structure of this region. Campillo and Plantet (1991) show that Q_{Lg} correlates with the heterogeneity of the lower crust in the Central Armorican Zone of Brittany, which is part of the Variscan Belt. The 1974 Lithospheric Seismic Profile of Britain (LISPB) includes a 700 km-long seismic reflection profile extending from off the north coast of Scotland to central England. It indicates strong variations in crustal structure in the Midland Valley/Southern Uplands region. While attenuation does increase south of the Highland Boundary Fault, the change is perhaps not as clear as expected but possibly not resolved by the data.

There is an indication from our results that the Laurentian terrains are associated with relatively low attenuation, as one would expect. The north-easternmost portion of the model is not well-resolved and it is not possible to assess the full extent of this zone. The collision zone region of the British Isles, defined here as extending from the Highland Boundary Fault in the north to the Flamborough Head Fault Zone in the south, is associated with relatively low Q at high frequencies ($f > 3$ Hz) but below 2.5 Hz, much of this region is characterised by relatively high Q. Zone 3, which is a region of relatively high Q observed at all frequencies does not correlate with any major structural feature or terrain. The massifs of Wales and South-western England are characterised by close to average attenuation at all frequencies. These parts of the study area are well sampled by the data so this is not due to the result being anchored to the starting model as it is in poorly

determined grid cells. The situation in the Irish Sea region (Zone 4) is also complex and high attenuation may be due to the presence of significant sedimentary deposits in this area. Further work is required to investigate the underlying mechanisms for the variation in crustal attenuation in Britain.

For earthquakes in Britain, including the offshore region, the method used to calculate ML is that of Hutton and Boore (1987) and uses their distance correction, which was developed for southern California. The results in Table 1 show that MW determined here is generally smaller than ML (by up to 0.9 magnitude units). Furthermore, the difference between ML and MW systematically increases with ML (Figure 10 c). Theoretically, ML should equal MW over the entire range for which ML can be determined (Deichmann, 2006). Differences between ML and MW are variously attributed to deficiencies in the path correction (e.g., Ristau et al. , 2003), changes in stress drop or rupture speed, or errors in the determination of ML for poorly recorded small earthquakes (Deichmann, 2006). Small earthquakes are more likely to have on-scale recordings at close distances compared with larger events on the low-gain networks that were in previously in operation in the UK. Therefore, it seems likely that the difference between ML and MW for British earthquakes is attributable to the distance correction used in the computation of ML.

We have done a number of tests to investigate the non-uniqueness between Q, the site and the source size term. The tomographic results remain very similar even when not inverting for site terms. We have also shown that a reasonable amount of noise can be added to the data without changing the results. A more serious issue as pointed out by (Menke, 2006) is the non-uniqueness between source term and Q. We computed null solutions for a constant synthetic Q model and the real data coverage by applying a perturbation to the source term, and then performing the tomographic inversion without source term. For a source term change of 0.1 moment magnitude units, which is similar to the standard deviation in our $M_W - M_L$ relation, the observed changes are of the order of $\delta Q^{-1} = 0.0001$ and thus less than the differences in the model obtained from the data, which is $\delta Q^{-1} = 0.0005$. If the non-uniqueness would equate to 0.2 magnitude units, the effect would be more severe. Overall, however, we conclude that the main features in the tomographic image are real as they are not easily seen in the results from the perturbation tests.

Despite using a very different model to Edwards et al. (2008), we obtain a very similar relationship

14   *S. Sargeant and L. Ottemöller*

between MW and ML. This indicates that the shear-wave displacement spectra can be modelled either with a relatively simple frequency-dependent Q model and assuming spherical spreading to 100 km and cylindrical spreading beyond that, as in this study or using a more complex model as in Edwards et al. (2008). The model of Edwards et al. (2008) employs depth-dependent, frequency-independent Q and a multi-segment geometrical spreading function. This highlights the non-uniqueness problem surrounding the formulation of the attenuation model itself. We prefer our simpler but possibly more physically realistic model, which gives very similar results.

7   CONCLUSIONS

Our study of Lg wave attenuation in Britain leads to the following conclusions:

(i) Average regional Q_{Lg} can be modelled as $266 f^{0.53}$.

(ii) Q_{Lg} varies spatially, with regions of lower than average attenuation in north-western Scotland, eastern central England, and south-western England. South-eastern England, the East Irish Sea Basin region and an area of eastern Scotland between the Southern Uplands Fault and the Highland Boundary Fault are characterised by higher than average attenuation.

(iii) The relationship between these regions and the gross tectonic structure of Britain does not seem to be straightforward and requires further investigation.

(iv) MW determined for 64 events using the regional average model is systematically lower than ML and the difference between MW and ML increases with ML.

8   ACKNOWLEDGEMENTS

References

Adams, J., & Haddon, R., 1998. Q for eastern North American Lg is a DECREASING function of frequency: contamination by Sn is to blame for the increasing function most researchers have found, *Seism. Res. Lett.*, **69**, 74.

Aki, K., 1967. Scaling law of seismic spectrum, *J. Geophys. Res.*, **72**, 1217-1231.

Aki, K., 1980. Attenuation of shear waves in the lithosphere for frequencies from 0.05 to 25 Hz, *Phys. Earth Planet. Int.*, **21**, 50–60.

Anderson, J. G. & Hough, S., 1984. A model for the shape of the Fourier amplitude spectrum of acceleration at high frequencies, *Bull. Seism. Soc. Am.*, **74**, 1969–1994.

Armstrong, H. A. & Owen, A. W., 2001. Terrane evolution of the paratectonic Caledonides of northern Britain, *J. geol. Soc. Lond.*, **158**, 475–486.

Atakan, K., Bard, P.-Y., Kind, F., Moreno, B., Roquette, P., Tento, A., the SESAME-team, 2004. J-SESAME: a standardized software solution for the H/V spectral ratio technique. *Proceedings of the 13th World Conference on Earthquake Engineering*, Vancouver, Canada, 1-6 August, 2004, paper no. 2270.

Bamford, D., Faber, S., Jacob, B., Kaminski, W., Nunn, K., Prodehl, C., Fuchs, K., King, R. & Willmore, P., 1976. A lithospheric seismic profile in Britain; I - preliminary results, *Geophys. J. Royal astr. Soc.*, **44**, 145–160.

Bamford, D., Nunn, K., Prodehl, C. & Jacob, B., 1978. LISPB-IV. Crustal structure of Northern Britain, *Geophys. J.R. astr. Soc.*, **54**, 43–60.

Barmin, M. P., Ritzwoller, M. H. & Levshin, A. L., 2001. A fast and reliable method for surface wave tomography, *Pure appl. Geophys.*, **158**, 1351–1375.

Barton, P. J., 1992. LISPB revisited: a new look under the Caledonides of northern Britain, *Geophys. J. Int.*, **110**, 371–391.

Baumgardt, D. R., 2001. Sedimentary basins and the blockage of Lg wave propagation in the continents, *Pure Appl. Geophys.*, **158**, 1207–1250.

Beamish, D. & Smythe, D. K., 1986. Geophysical images of the deep crust: the Iapetus Suture, *J. geol. Soc. Lond.*, **143**, 489–497.

Benz, H. M., Frankel. A. & Boore, D. M., 1997. Regional Lg attenuation for the continental United States, *Bull. seism. Soc. Am.*, **87**, 606–619.

Bluck, B. J., 1984. Pre-Carboniferous history of the Midland Valley of Scotland, *Trans. R. Soc.*

16   *S. Sargeant and L. Ottemöller*

Edin. Earth Sci., **75**. 275–296.

Bluck, B. J., 2000. Old Red Sandstone basins and alluvial systems of Midland Scotland. In Friend, P.F. & Williams, B.P.J. (eds), New Perspectives on the Old Red Sandstone, *Geol. Soc. Lond. Spec. Pub.*, **180**, 417–437.

Bluck, B. J., 2002. The Midland Valley terrane. In Trewin, N.H. (ed) *The Geology of Scotland* (4th Edition), 149–166, The Geological Society of London.

Booth, D. C., 2007. An improved UK local magnitude scale from analysis of shear- and Lg-wave amplitudes, *Geophysical Journal International*, **169**, 593–601.

Bowman, J. R., & Kennett, B. L. N., 1991. Propagation of Lg waves in the North Australian craton: influence of crustal velocity gradients, *Bull. seism. Soc. Am.*, **81**, 592–610.

British Geological Survey, 1996. *Tectonic map of Britain, Ireland and adjacent areas*. Pharaoh, T., Morris, J. H., Long, C. B., and P. D. Ryan (compilers), 1:1 500 000 (Keyworth, Nottingham, UK).

Brune, J. N., 1970. Tectonic stress and the spectra of seismic shear waves from earthquakes, *J. Geophys. Res.*, **75**, 4997–5009.

Brune, J. N., 1971. Correction, *J. Geophys. Res.*, **76**, 5002.

Campillo, M., Plantet, J. L. & Bouchon, M., 1985. Frequency dependent attenuation in the crust beneath Central France from Lg waves: data analysis and numerical modelling, *Bull. seism. Soc. Am.*, **75**, 1395–1411.

Campillo, M., 1987. Lg wave propagation in a laterally varying crust and the distribution of quality factor in Central France, *J. geophys. Res.*, **92**, 12604–12614.

Campillo, M. & Plantet, J. L., 1991. Frequency dependence and spatial distribution of seismic attenuation in France: experimental results and possible interpretations, *Phys. Earth planet. Int.*, **67**, 48–64.

Chadwick, R. A. & Pharaoh, T. C., 1998. The seismic reflection Moho beneath the United Kingdom and adjacent areas, *Tectonophysics*, **299**, 255–279.

Clegg, B. & England, R., 2003. Velocity structure of the UK continental shelf from a compilation of wide-angle and refraction data, *Geol. Mag.*, **140**, 453–467.

Clegg, P. & Holdsworth, R. E., 2005. Complex deformation as a result of strain partitioning in transpression zones: an example from the Leinster terrane, SE Ireland, *J. geol. Soc. Lond.*, **162**, 187–202.

Cocks, L. R. M., McKerrow, W. S. & van Staal, C. R., 1997. The margins of Avalonia, *Geol. Mag.*, **134**, 627–636.

Cocks, L. R. M., 2005. Presidential address 2005: where was Britain in the Palaeozoic?, *Proc. Geol. Ass.*, **116**, 117–127.

Deichmann, N., 2006. Local magnitude, a moment revisited, *Bull. seism. Soc. Am.*, **96**, 1267–1277.

Edwards, B., Rietbrock, A., Bommer, J. J., & Baptie, B., 2008. The acquisition of source, path, and site effects from microearthquake recordings using Q tomography: application to the United Kingdom, *Bull. seism. Soc. Am.*, **98**, 1915–1935.

Fedotov, S. A. & Boldyrev, S. A., 1969. Frequency dependence of body-wave absorption in the crust and upper mantle of the Kuril Islands chain, Izv. Akad. Sci. USSR, *Phys. Solid Earth*, **9**, 17–33.

Furumura, T. & Kennett, B. L. N., 1997. On the nature of regional seismic phases - II. On the influence of structural barriers, *Geophys. J. Int.*, **129**, 221–234.

Green, P. F., Thomson, K. & Hudson, J. D., 2001. Recognition of tectonic events in undeformed regions: contrasting results from the Midland Platform and East Midlands Shelf, *J. geol. Soc. Lond.*, **158**, 59-73.

Gregersen, S. & Vaccari, F., 1993. Lg-wave modelling for the North Sea, *Geophys. J. Int.*, **114**, 76–80.

Hermann, R. B., and Kijko, A., 1983, Modeling some empirical Lg relations, *Bull. Seism. Soc. Am.*, **56**, 167–172.

Hutton, L. K. & Boore, D. M., 1987. The ML scale in southern California, *Bull. seism. Soc. Am.*, **77**, 2074–2094.

Kennett, B. L. N., 1986. Lg waves and structural boundaries, *Bull. seism. Soc. Am.*, **76**, 1133–1141.

Kennett, B. L. N. & Mykkeltveit, S., 1984. Guided wave propagation in laterally varying media - II. Lg-waves in north-western Europe, *Geophys. J. R. astr. Soc.*, **79**, 257–267.

Konno, K., Ohmachi, T., 1998. Ground-motion characteristics estimated from spectral ratio between horizontal and vertical components of microtremor, *Bull. Seism. Soc. Am.*, **88**, 228–241.

Kvamme, L. B., Hansen, R. A. & Bungum, H., 1995. Seismic-source and wave-propagation effects of Lg waves in Scandinavia, *Geophys. J. Int.*, **120**, 525–536.

Leggett, J. K., McKerrow, W. S. & Casey, D. M., 1982. The anatomy of a Lower Palaeozoic accretionary fore-arc: the Southern Upland of Scotland. In Leggett, J. K. (ed) Trench-fore-arc geology, *Geol. Soc. Lond. Spec. Pub.*, **10**.

MacBeth, C. D. & Burton, P. W., 1987. Single-station attenuation measurements of high-

18   *S. Sargeant and L. Ottemöller*

frequency Rayleigh waves in Scotland, *Geophys. J. R. astr. Soc.*, **89**, 757–797.

Marrow, P. C., 1992. UK earthquake magnitudes: A comparison of methods and published results, *BGS Technical Report* WL/92/36.

Menke, W., Holmes, R. C. & Xie, J., 2006. On the nonuniqueness of the coupled origin time-velocity tomography problem, *Bull. seis. soc. Am.*, **96**, 1131–1139.

McNamara, D. E. & Walter, W. R., 2001. Mapping crustal heterogeneity using Lg propagation efficiency throughout the Middle East, Mediterranean, southern Europe and northern Africa, *Pure appl. Geophys.*, **158**, 1165–1188.

Mitchell, B. J., Baqer, S., Akinci, A. & Cong, L., 1998. Lg coda Q in Australia and its relation to crustal structure and evolution, *Pure. appl. Geophys.*, **153**, 639–653.

Mitchell, B. J. & Hwang, H. J., 1987. Effect of low Q sediments and crustal Q on Lg attenuation in the United States, *Bull. seism. Soc. Am.*, **77**, 1197–1210.

Nakamura, Y., 1989. A method for dynamic characteristics estimation of subsurface using microtremor on the ground surface, *QR of RTRI*, **30**, 25–33.

Noghoshi, M., Igarashi, T., 1970. On the propagation characteristics of microtremors, *J. Seism. Soc. Japan*, **23**, 264–280, (in Japanese with English abstract).

Noghoshi, M., Igarashi, T., 1971. On the amplitude characteristics of microtremors, *J. Seism. Soc. Japan*, **24**, 24–40, (in Japanese with English abstract).

Ojeda, A. & Ottemöller, L., 2002. Q_{Lg} tomography in Colombia, *Phys. Earth planet. Int.*, **130**, 253–270.

Ottemöller, L., Shapiro, N. M., Singh, S. K. & Pacheco, J. F., 2002. Lateral variation of Lg wave propagation in southern Mexico, *J. geophys. Res.*, **107**, 10.1029/2001JB000206.

Ottemöller, L., 2002. Lg wave Q tomography in Central America, *Geophys. J. Int.*, **150**, 295–303.

Ottemöller, L. & Havskov, J., 2003. Moment magnitude determination for local and regional earthquakes based on source spectra, *Bull. Seism. Soc. Am.*, **93**, 203–214.

Ottemöller, L. & Thomas, C., 2006. Highland Boundary Fault Zone: tectonic implications of the Aberfoyle earthquake sequence of 2003, submitted.

Pharaoh, T., England, P. & Lee, M., 1995. The concealed Caledonide basement of eastern England and the southern North Sea - a review, *Studia geoph. et geod.*, **39**, 330–346.

Phillips, E. R., Smith, R. A. & Carroll, S., 1998. Strike-slip, terrane accretion and the pre-Carboniferous evolution of the Midland Valley of Scotland, *Trans. R. Soc. Edin. Earth Sci.*, **89**, 209–224.

Richter, C. F., 1935. An instrumental earthquake magnitude scale, *Bull. Seism. Soc. Am.*, **25**,

1–32.

Ristau, J., Rogers, G. C. & Cassidy, J. F., 2003. Moment magnitude - local magnitude calibration for earthquakes off Canada's west coast, *Bull. seism. Soc. Am.*, **93**, 2296–2300.

Scheirer, D. S. & Hobbs, R. W., 1990. Seismic attenuation in the continental crust SW of England, *Geophys. J. Int.*, **103**, 533–540.

SESAME, 2004. Guidelines for the implementation of the H/V spectral ratio technique on ambient vibrations - measurements, processing and interpretation, SESAME European research project WP12 Deliverable D23.12. Tech. rep., European Commission Research General Directorate Project No. EVG1-CT-2000-00026 SESAME.

Shi, J., Young, K.-W. & Richards, P. G., 1996. Variability of crustal attenuation in the northeastern United States from Lg waves, *Geophys. J. Int.*, **101**, 23231–25242.

Shin, T.-C. & Herrmann, R. B., 1987. Lg attenuation and source studies using 1982 Miramichi data, *Bull. seism. Soc. Am.*, **77**, 384–397.

Soper, N. J., Gibbons, W. & McKerrow, W. S., 1989. Displaced terranes in Britain and Ireland, *J. geol. Soc. Lond.*, **146**, 365–367.

Sørensen, M. B., Oprsal, I., Bonnefoy-Claudet, S., Atakan, K., Mai, P. M., Pulido, N., Yalciner, C., 2006. Local site effects in Ataköy, Istanbul, Turkey, due to a future large earthquake in the Marmara Sea. *Geophys. J. Int.*, **167**, 1413–1424.

Stone, P., Floyd, J. D., Barnes, R. P. & Lintern, B. C., 1987. A sequential back-arc and foreland basin thrust duplex model for the Southern Uplands of Scotland, *J. geol. Soc. Lond.*, **144**, 753–64.

Stone, P. & Merriman, R. J., 2004. Basin thermal history favours an accretionary origin for the Southern Uplands terrane, Scottish Caledonides, *J. geol. Soc. Lond.*, **161**, 829–836.

Vesnaver, A. & Böhm, G., 2000. Staggered or adapted grids for seismic tomography?, *The Leading Edge*, **19**, 944–950.

Woodcock, N. & R. Strachan, 2000. *Geological History of Britain and Ireland*, Blackwell Publishing, Oxford, UK, 432 p.

20   *S. Sargeant and L. Ottemöller*

Year	Month	Day	Lat (° N)	Lon (° E)	Depth (km)	ML	MW	σ	N
1981	10	27	54.15	0.3	23.7	3.7	2.9	0	1
1984	4	15	52.42	-3.23	10.6	3.3	3	0.1	8
1984	7	29	52.98	-4.44	21.2	4	3.5	0.1	12
1984	7	30	52.97	-4.38	20	2.8	2.5	0.1	3
1984	8	4	52.97	-4.4	24.1	2.7	2.9	0.1	4
1984	8	6	52.95	-4.33	24.7	3.6	3.3	0.2	3
1984	8	18	52.96	-4.38	21	4.3	3.8	0.1	7
1985	12	1	57.03	-5.77	4.2	3.7	3.1	0.2	7
1986	9	29	56.45	-5.65	23.3	4.1	3.4	0.2	14
1986	12	26	51.9	-1.34	23.5	2.9	2.7	0.1	3
1987	10	4	57.98	-5.2	0.4	3	3	0.2	14
1987	10	4	57.97	-5.19	0.5	3	2.9	0.1	8
1987	10	17	57.93	-5.14	2	2.9	2.9	0.2	3
1990	1	26	56	-6.57	9.2	3	2.6	0.1	8
1990	2	8	53.52	-1.16	17.9	3	2.9	0.1	5
1991	12	14	50.65	1.86	0.4	3.6	3.1	0.1	7
1992	1	27	50.66	1.88	7.3	3	2.6	0.1	3
1992	2	17	52.5	-0.19	11.1	3.3	2.9	0.1	20
1992	7	26	57.49	-5.66	15.1	2.8	2.7	0.2	11
1992	7	29	53.13	-4.4	11.3	3.5	2.9	0.1	20
1993	6	26	54.21	-2.86	8.3	3	3	0.1	29
1993	7	12	53.74	1.37	7.4	2.9	2.8	0.1	13
1993	9	4	57.03	-5.78	2.6	2.7	2.5	0.1	14
1994	1	1	51.36	-3.57	14.7	2.8	2.9	0.2	18
1994	2	10	53.21	-4.14	14	2.9	2.7	0.1	17
1994	2	15	52.56	0.91	7.3	4	3.4	0.1	18
1994	2	15	52.56	0.93	2.5	2.8	2.5	0.1	11
1994	3	17	52.54	-3.44	21.6	3.1	3	0.2	8
1994	5	12	52.15	-1.74	15.9	3	3	0.1	20
1994	8	17	57.19	-5.73	3	3.1	2.8	0.2	16

Year	Month	Day	Lat (° N)	Lon (° E)	Depth (km)	ML	MW	σ	N
1994	9	15	51.8	1.8	8	3.2	3	0.1	10
1995	8	17	49.88	-4.26	11.1	3.1	2.7	0.1	10
1996	3	7	52.8	-2.74	10.4	3.2	3	0.2	22
1996	9	20	52.32	-3.33	14.4	2.9	2.5	0.1	7
1996	11	10	50	-5.58	8.3	3.6	3.2	0.2	24
1998	5	3	56.06	-6.05	12.9	3.1	3.1	0.1	27
1998	5	16	53.02	2.16	0.2	3.8	3.4	0.2	26
1999	1	21	53.09	0.07	16.9	2.8	2.7	0.1	5
1999	3	4	55.4	-5.24	19	4	3.2	0.1	25
1999	9	1	53.2	-4.35	16.3	3.2	2.9	0.2	24
1999	10	25	51.97	-3.57	14.1	3.6	3.3	0.2	20
2000	9	23	52.28	-1.61	14.4	4.2	3.3	0.1	20
2000	12	21	53.52	1.85	8.6	3.3	3.3	0.3	10
2001	5	13	55.1	-3.64	11.5	3	2.9	0.1	33
2001	5	31	50.98	-4.53	26.4	3.6	3.2	0.1	17
2001	10	10	51.7	-3.26	6.5	3.1	2.8	0.2	20
2001	10	28	52.85	-0.86	11.6	4.1	3.4	0.1	19
2002	2	12	51.7	-3.26	5.2	3	2.6	0.2	17
2002	6	20	51.57	-3.08	14.3	2.9	2.8	0	6
2002	9	22	52.53	-2.16	14	4.7	4.2	0.1	12
2002	9	30	48.08	-3.23	21.7	4.5	4.2	0.2	13
2002	10	21	53.48	-2.2	5	3.2	2.9	0.2	28
2002	10	22	53.47	-2.15	4.2	2.9	2.9	0.2	24
2002	10	24	53.49	-2.18	3.7	3.1	3	0.2	27
2003	6	20	56.17	-4.43	5.2	3.2	2.8	0.2	15
2003	8	19	53.48	-1.01	13.2	3.1	2.6	0.2	13
2004	1	29	51.09	-2.98	6.5	3.1	2.8	0.2	8
2004	2	29	53.57	-2	12.4	3.1	2.7	0.2	22
2005	12	14	53	-5.64	10	2.8	2.7	0.1	7
2005	12	23	56.68	-5.69	6.7	2.7	2.5	0.2	9

22   *S. Sargeant and L. Ottemöller*

Year	Month	Day	Lat (° N)	Lon (° E)	Depth (km)	ML	MW	σ	N
2006	6	8	57.53	-5.64	8.3	2.9	2.6	0.1	5
2006	12	26	55.09	-3.63	7.5	3.5	3.2	0.1	12
2007	1	23	51.66	2.1	15	3.5	3.3	0.1	6
2007	4	28	51.08	1.17	2	4.3	3.7	0.1	14

Table 1Earthquakes in the dataset (including moment magnitudes determined from spectral modelling. σ is the standard deviation on MW and N is the number of observations used. ML is the local magnitude published by BGS.
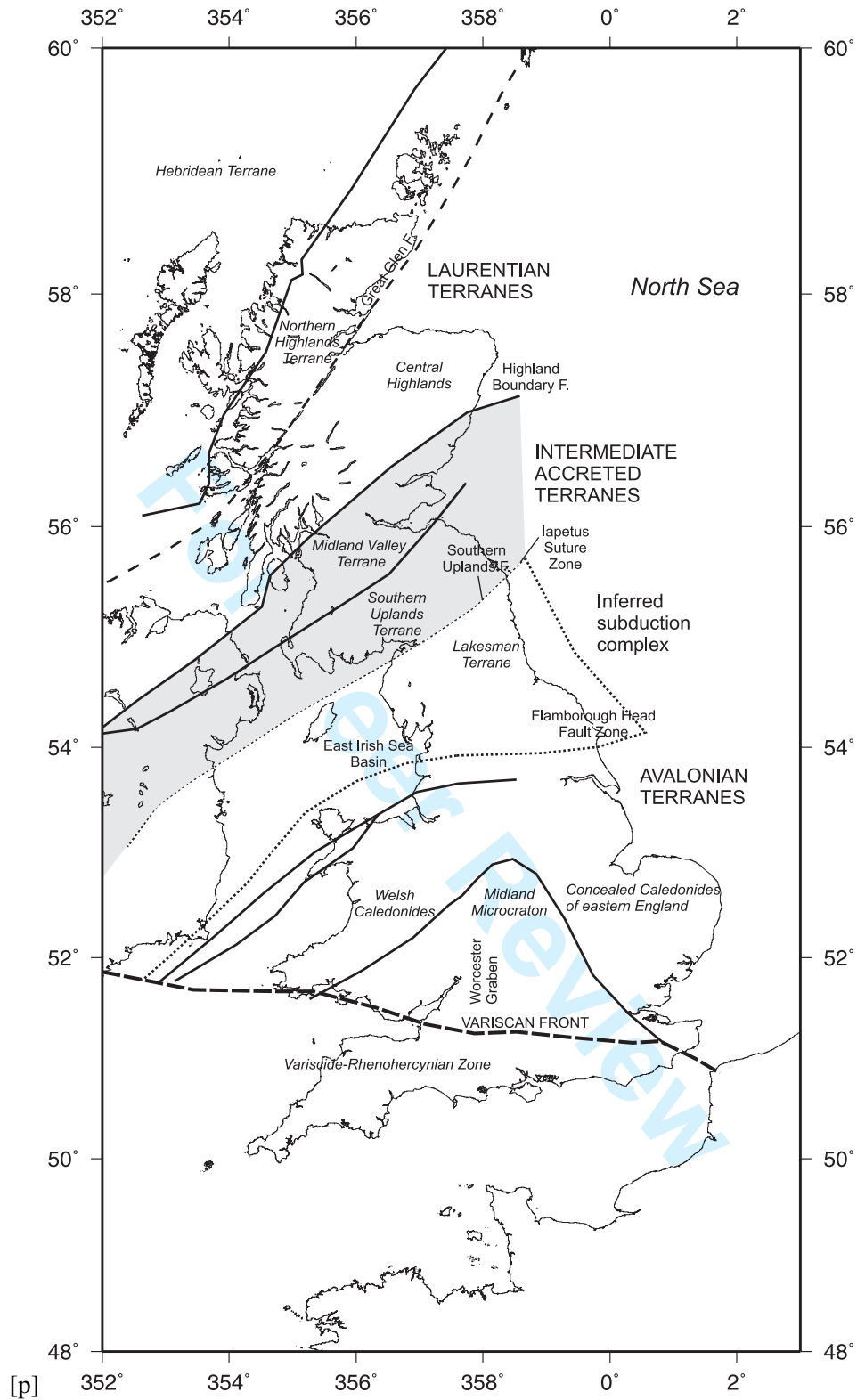
Figure 1. Basic tectonic map of the British Isles showing the main terrains (in italics), and other key structures (after British Geological Survey, 1996).

24   *S. Sargeant and L. Ottemöller*
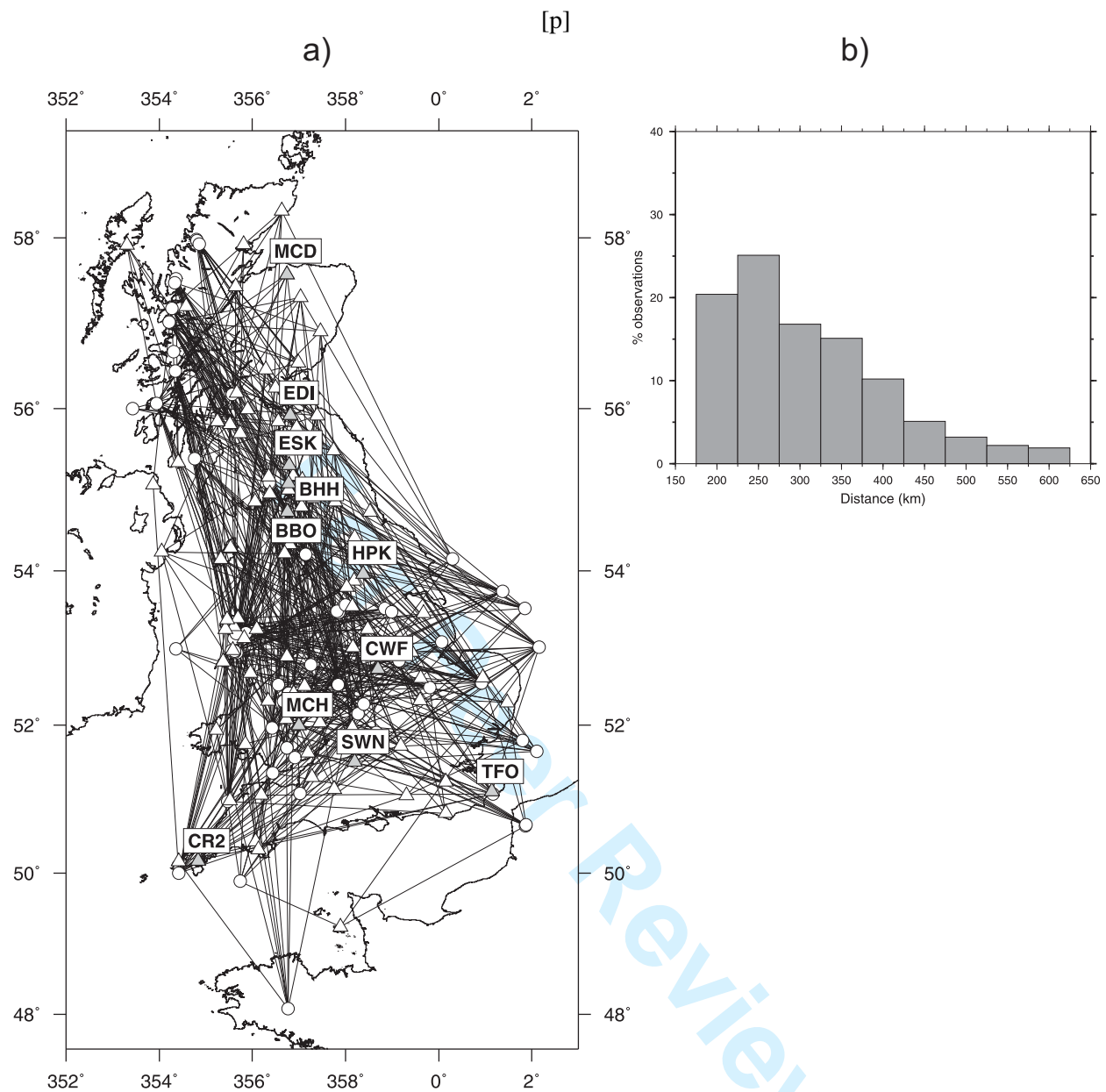
Figure 2. a) Source-station pairs used to determine Q_{Lg}^{-1}. Triangles are seismological stations. Circles denote earthquake epicentral locations. Three-component stations for which H/V spectral ratios were investigated (see Figure 7) are labelled, b) Distribution of observations with distance.

[p]
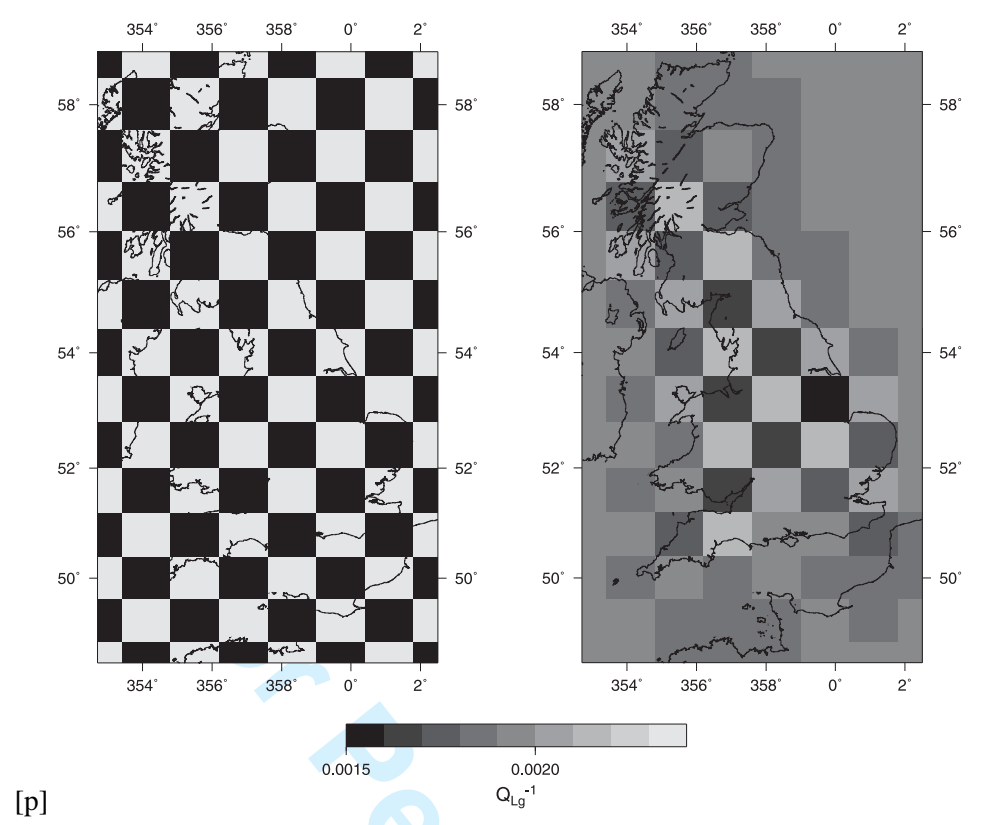
Figure 3. Results from the checkerboard test at 3.6 Hz using the parameters discussed in Section 4.

26   *S. Sargeant and L. Ottemöller*

[p]
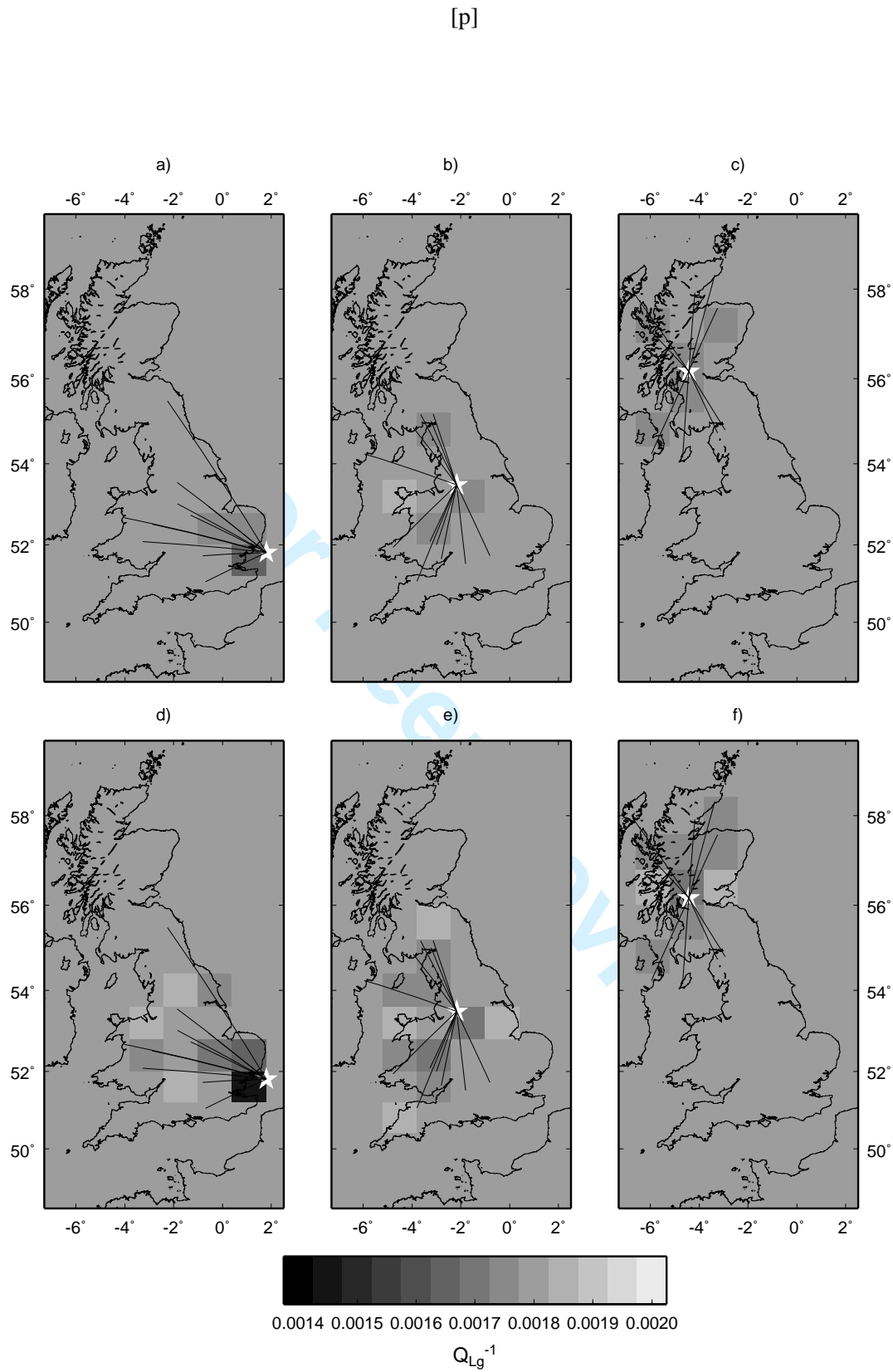
Figure 4. Results from source size perturbation test. One of the earthquake source terms is changed by 0.1 (a, b, c) or 0.2 (d, e, f) moment magnitude units and the inversion for Q_{Lg}^{-1} is done for a synthetic model with constant Q based on the real data path distribution. The same earthquake is perturbed in plots a and d, b and e, and c and f.
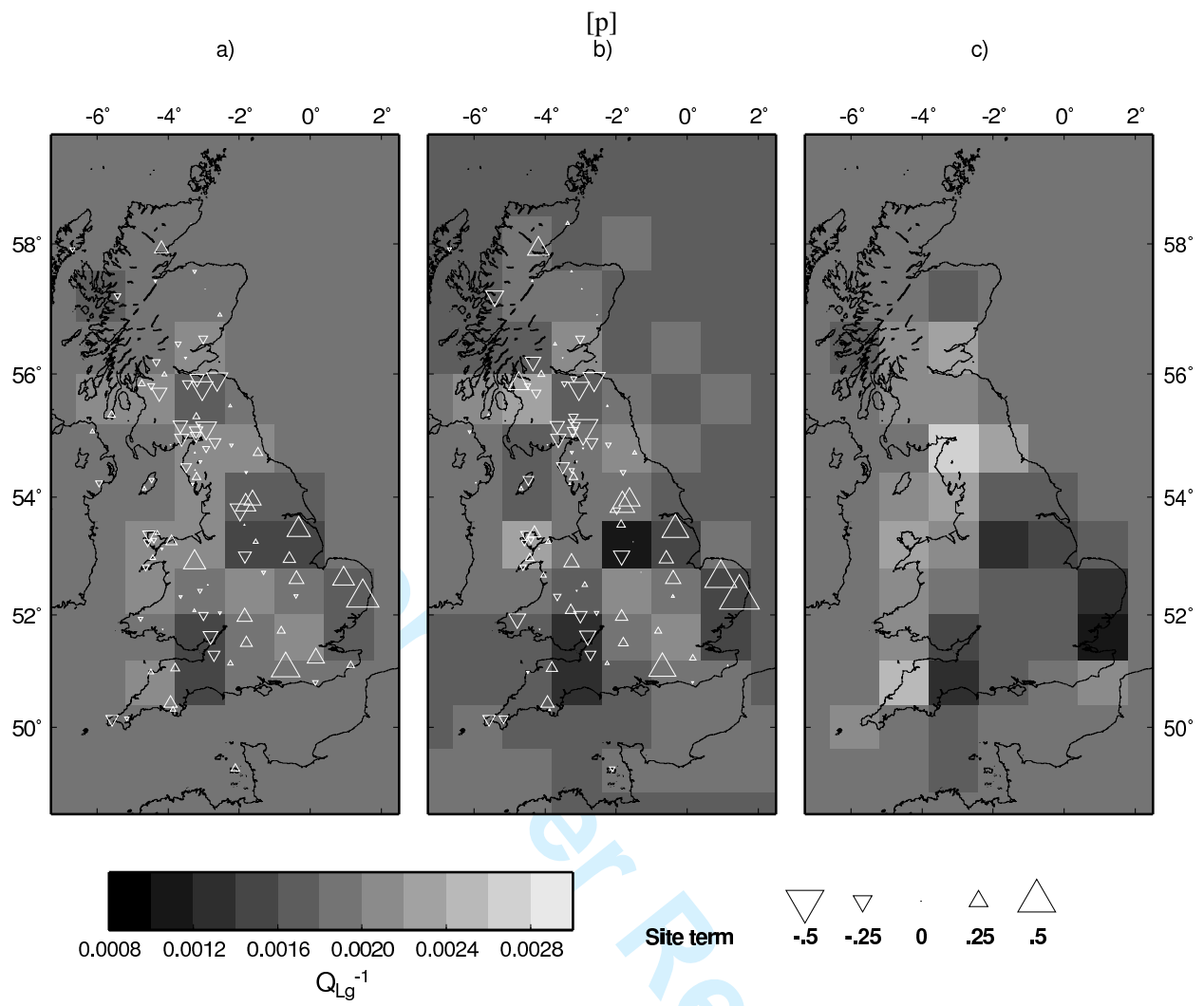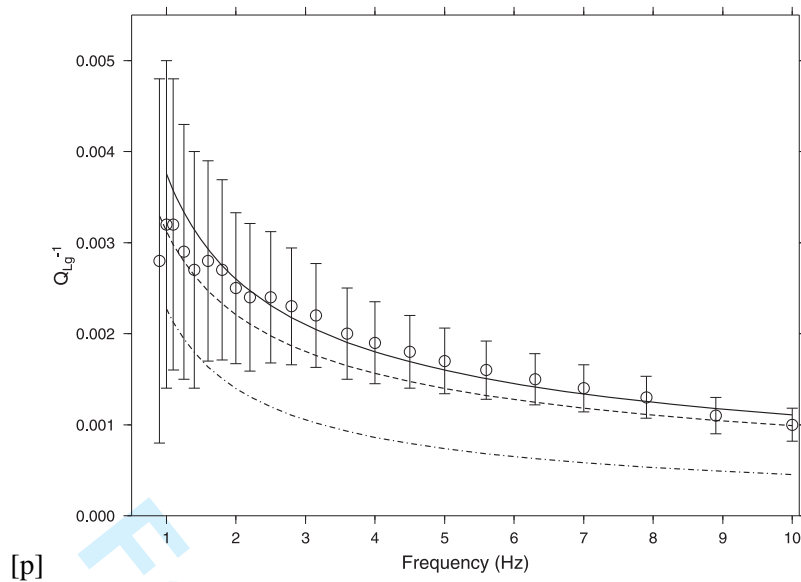
Figure 5. Results from tomographic inversion for a frequency of 4 Hz: a) Inversion for Q^{-1} and site terms, b) inversion for Q^{-1} and site terms after adding Gaussian noise to the data equivalent to 0.1 moment magnitude units and c) Inversion for Q^{-1} without site terms.

28   *S. Sargeant and L. Ottemöller*

[p]

Figure 6. Regional average Q_{Lg}^{-1} model for Britain as a function of frequency. The circles represent average Q_{Lg}^{-1} values obtained in the inversion. The solid line is the model based on these observations. For comparison, the relations for France (dashed line) proposed by Campillo and Plantet (1991) and Scandinavia (dotted line) presented by Kvamme et al. (1995) are also shown.

[p]
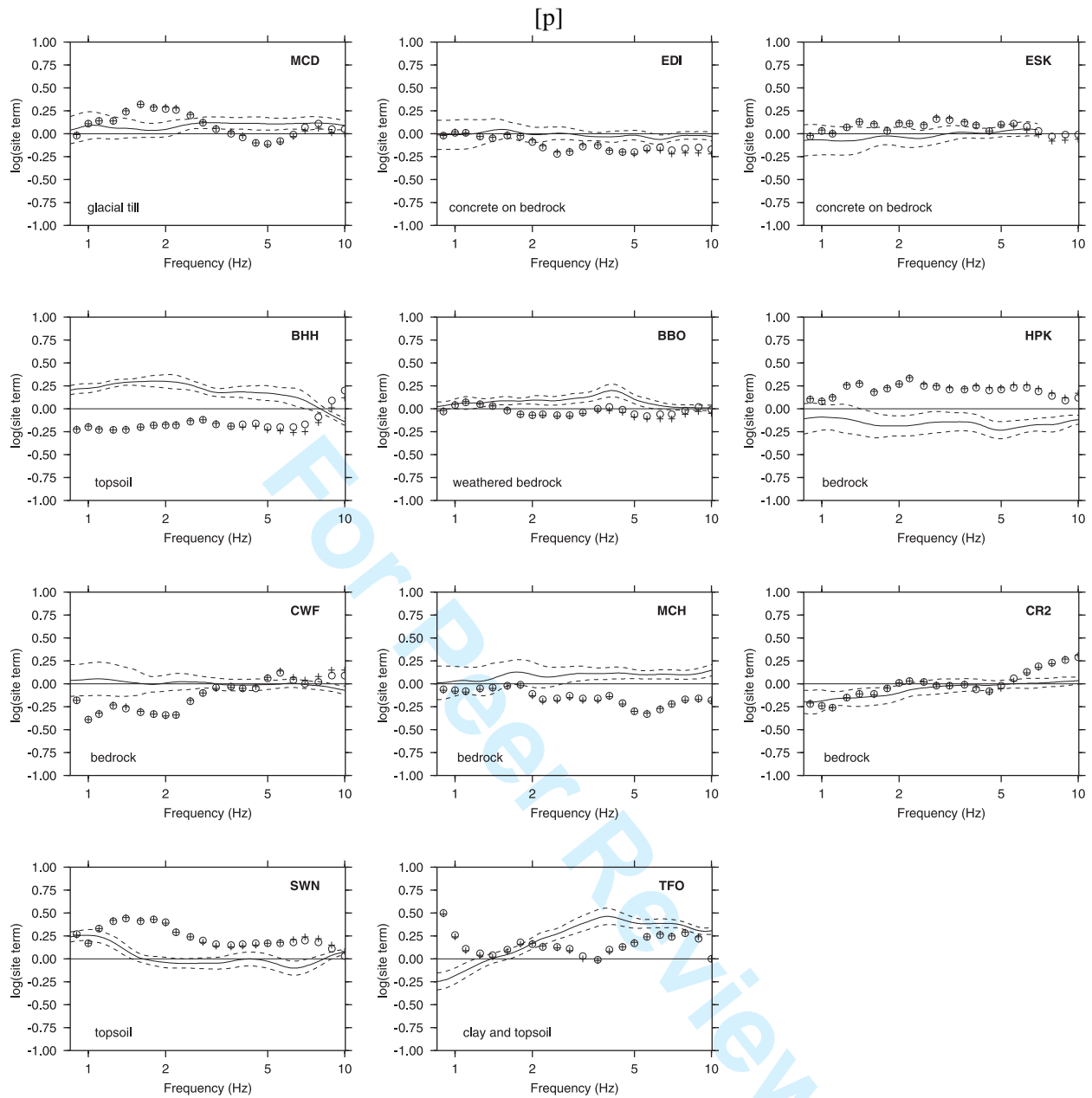
Figure 7. Site terms obtained in the average (crosses) and tomography (circles) inversions. Results from the H/V spectral ratio technique are also shown: solid line is the mean, dashed lines correspond to plus and minus one standard deviation from the mean. The shallow geology at site is also given (bottom left). The stations are labelled in Figure 2.
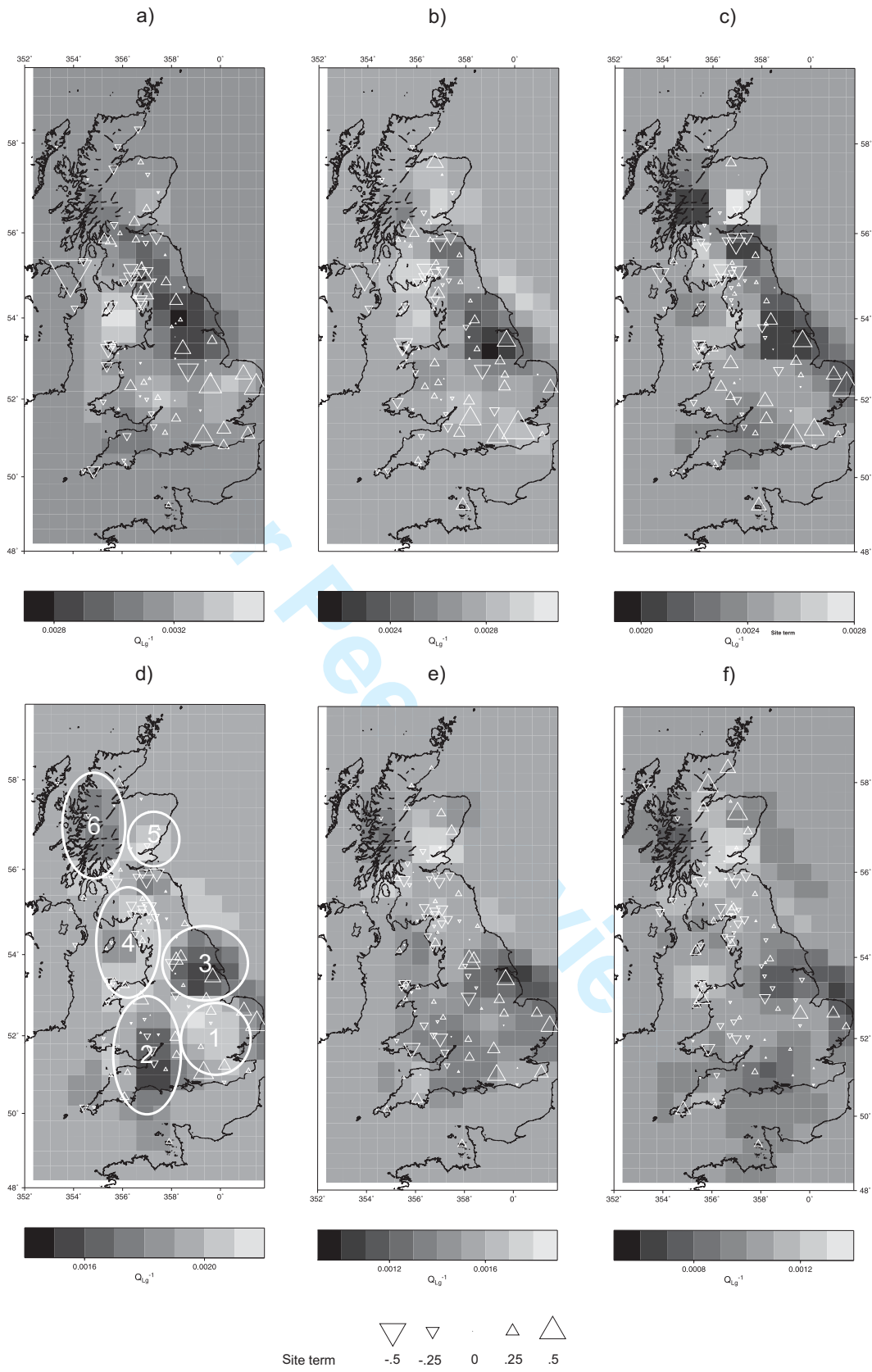
30   *S. Sargeant and L. Ottemöller*

Figure 8. Tomographic inversion results for Q_{Lg}^{-1} at a) 1.0 Hz, b) 1.6 Hz, c) 2.5 Hz, d) 4.0 Hz, e) 6.3 Hz and f) 10.0 Hz.
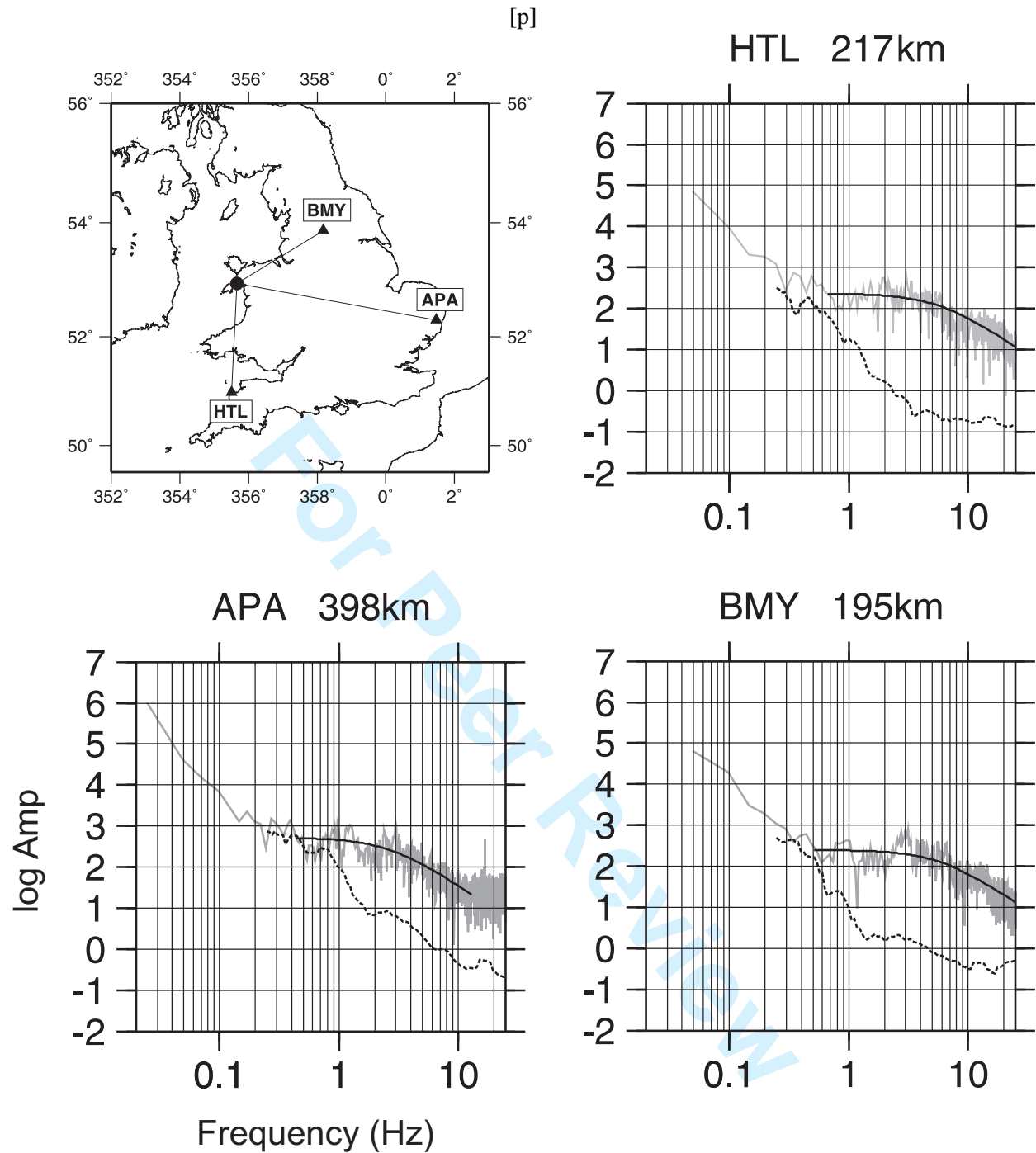
Figure 9. Typical spectral modelling results for the Mw 3.3 event of 6 August 1984. The grey lines show the observed source spectra, the black solid lines show the theoretical spectra based on the results of the modelling (note that the theoretical spectra are only shown for the frequency range used in the grid search). The dashed lines show the noise spectrum taken from before the P arrival.
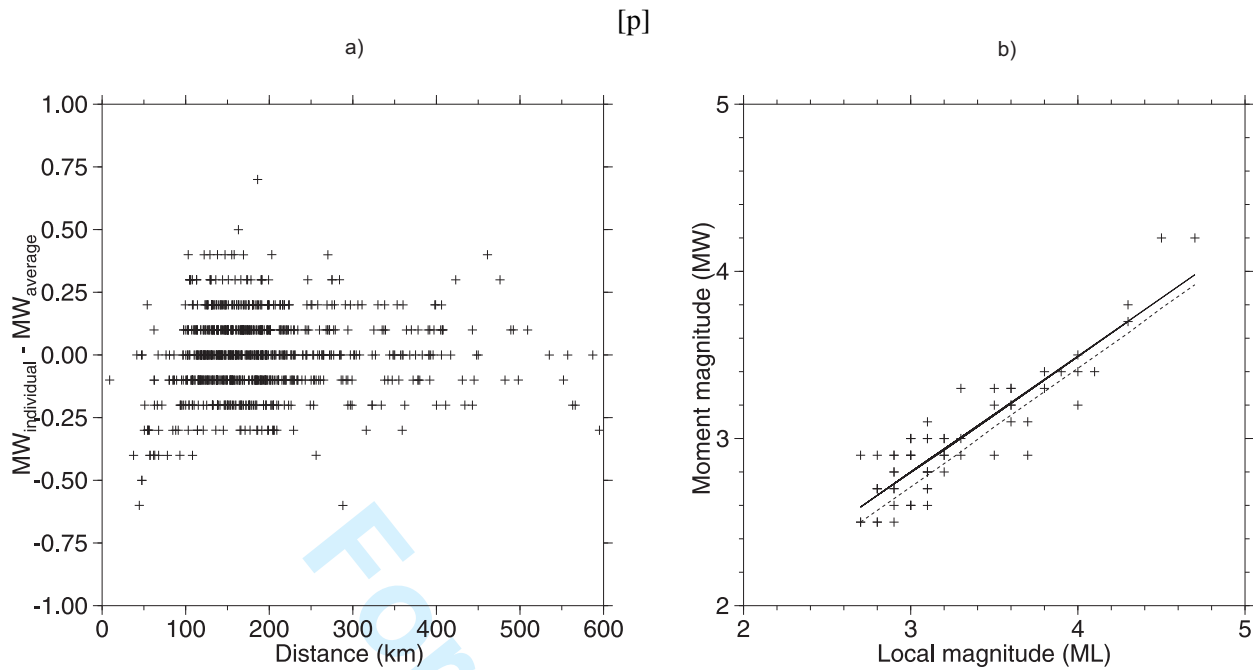
32   *S. Sargeant and L. Ottemöller*

[p]

a)   b)

Figure 10. a) Difference between MW calculated for single station spectra and average MW determined for each event (Table 1) plotted against distance. b)MW vs. ML where MW was determined using the average Q_{Lg}^{-1} model found here. Solid line - MW computed using equation 7, dashed line - MW computed using Edwards et al. (2008).